

## Supporting Information

# Vapor-Infiltration Approach Towards Selenium/Reduced Graphene Oxide Composites Enabling Stable and High-Capacity Sodium Storage

*Xuming Yang,<sup>a,b</sup> Jinkai Wang,<sup>c</sup> Shuo Wang,<sup>d</sup> Hongkang Wang,<sup>c</sup> Ondrej Tomanec,<sup>e</sup> Chunyi Zhi,<sup>a</sup>  
Radek Zboril,<sup>e</sup> Denis Y. W. Yu\*,<sup>d</sup> Andrey Rogach\*<sup>a,b</sup>*

<sup>a</sup>Department of Materials Science and Engineering, City University of Hong Kong, 83 Tat Chee Avenue, Kowloon, Hong Kong S.A.R.

<sup>b</sup>Center for Functional Photonics (CFP), City University of Hong Kong, 83 Tat Chee Avenue, Kowloon, Hong Kong S.A.R.

<sup>c</sup>Center of Nanomaterials for Renewable Energy (CNRE), State Key Lab of Electrical Insulation and Power Equipment, School of Electrical Engineering, Xi'an Jiaotong University, Xi'an, China

<sup>d</sup>School of Energy and Environment, and Center of Super-Diamond and Advanced Films (COSDAF), City University of Hong Kong, 83 Tat Chee Avenue, Kowloon, Hong Kong S.A.R.

<sup>e</sup>Regional Centre of Advanced Technologies and Materials, Faculty of Science, Department of Physical Chemistry, Palacky University in Olomouc, 77146 Olomouc, Czech Republic

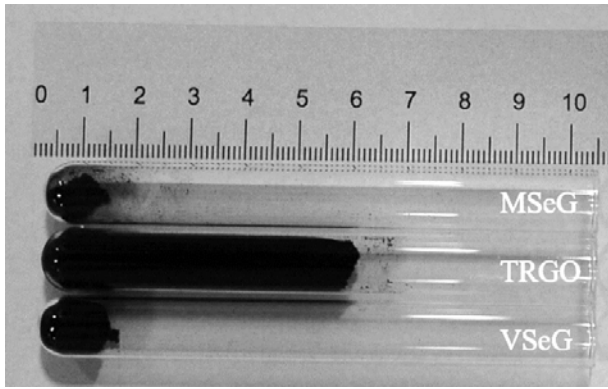


Figure S1. Digital photos of MSeG, TRGO and VSeG with the same weight of 30 mg showing large difference in volume.

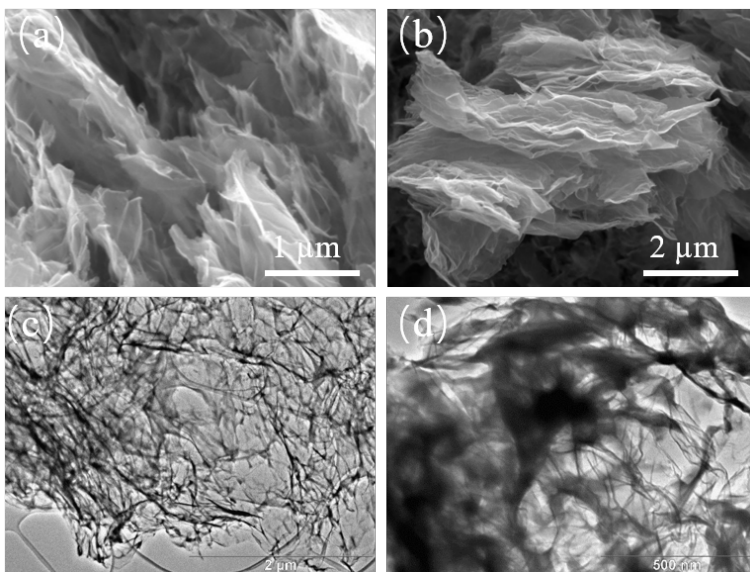


Figure S2. SEM images of (a) MSeG and (b) VSeG; TEM images of (c) TRGO and (d) MSeG.

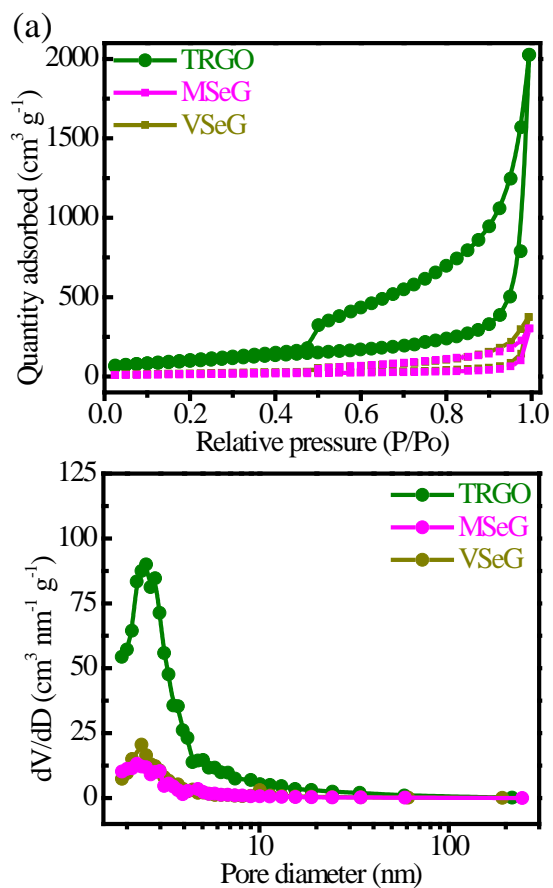


Figure S3. (a) Nitrogen adsorption-desorption isotherms and (b) pore size distribution of TRGO, MSeG and VSeG.

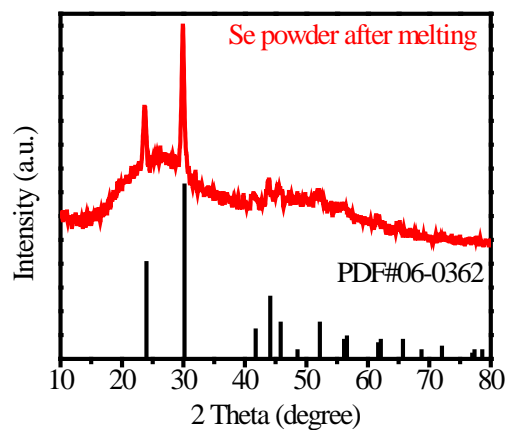


Figure S4. XRD pattern of Se powder after annealed at 260 °C for 12 hours.

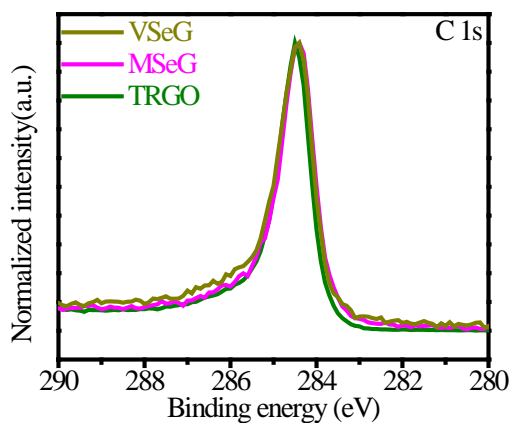


Figure S5. Core-level C 1s XPS spectra of GO, TRGO, MSeG and VSeG.

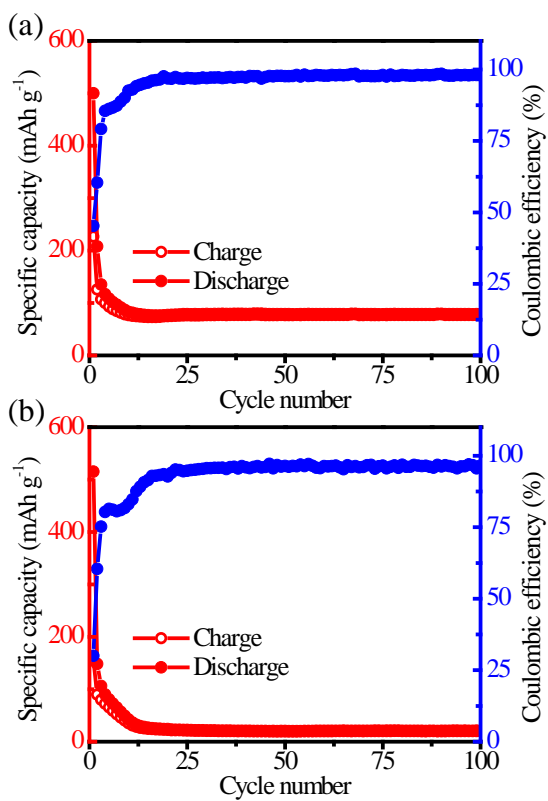


Figure S6. Cycle performance of (a) VSeG and (b) MSeG in PC electrolyte.

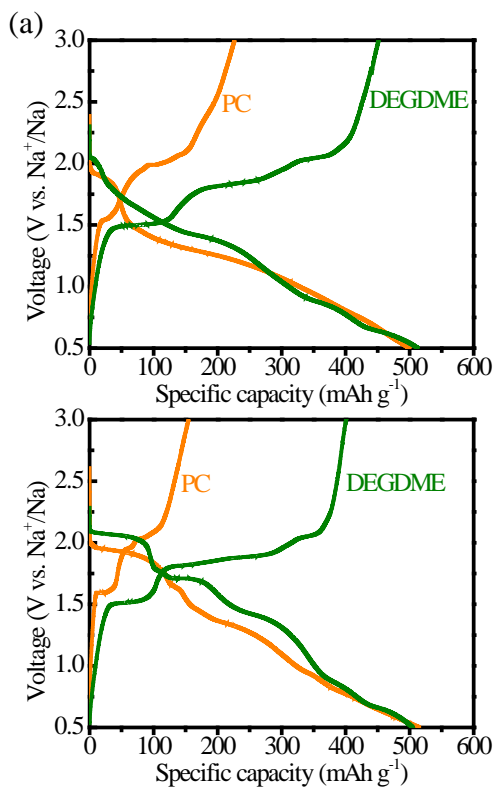


Figure S7. Voltage profiles of (a) Na-MSeG and (b) Na-VSeG cells with PC and DEGDME electrolytes.

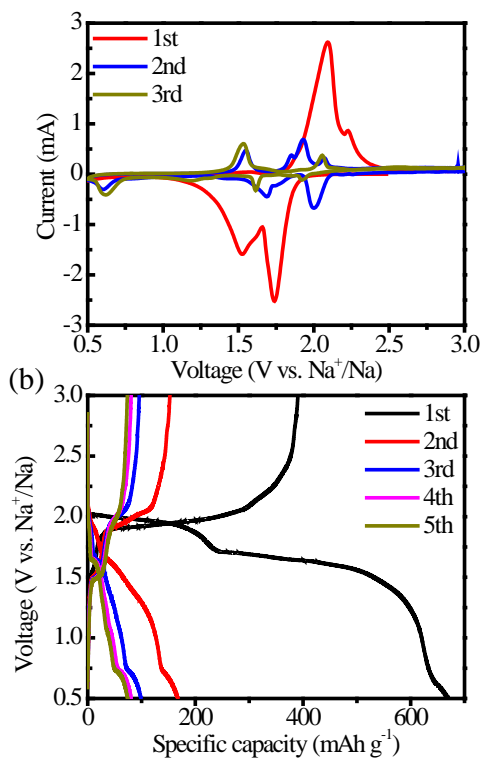


Figure S8. (a) Cyclic voltammograms at  $0.2 \text{ mV s}^{-1}$  and (b) voltage profiles of Se powder at  $0.1 \text{ A g}^{-1}$  in the ether electrolyte.

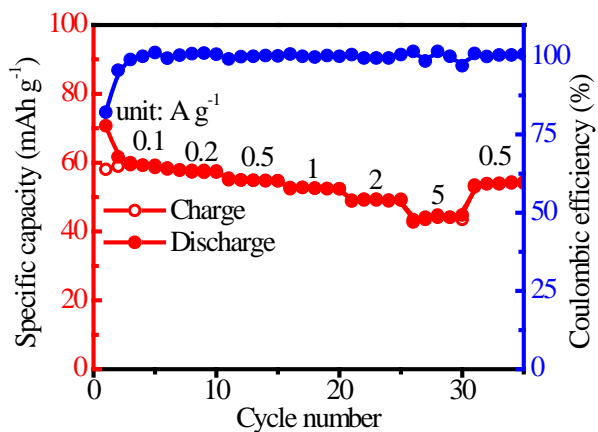


Figure S9. Sodium storage performance of TRGO within the voltage range of 0.5~3.0 V.

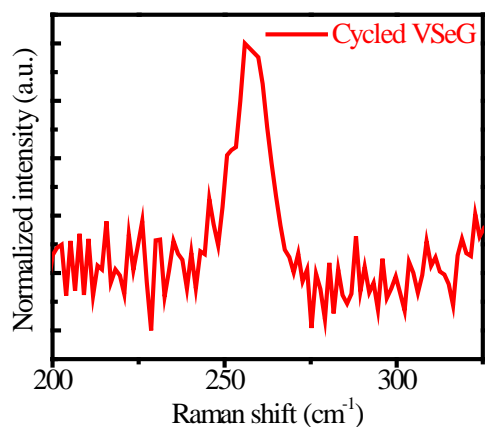


Figure S10. Raman spectrum of cycled VSeG electrode.

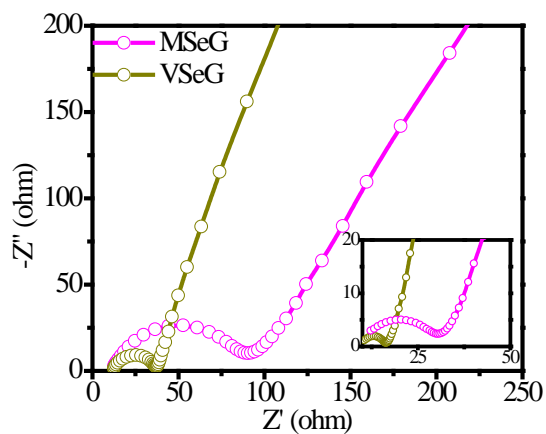


Figure S11. Electrochemical impedance spectrum of MSeG and VSeG at initial states and after one cycle at 0.1 A g<sup>-1</sup> (inset).

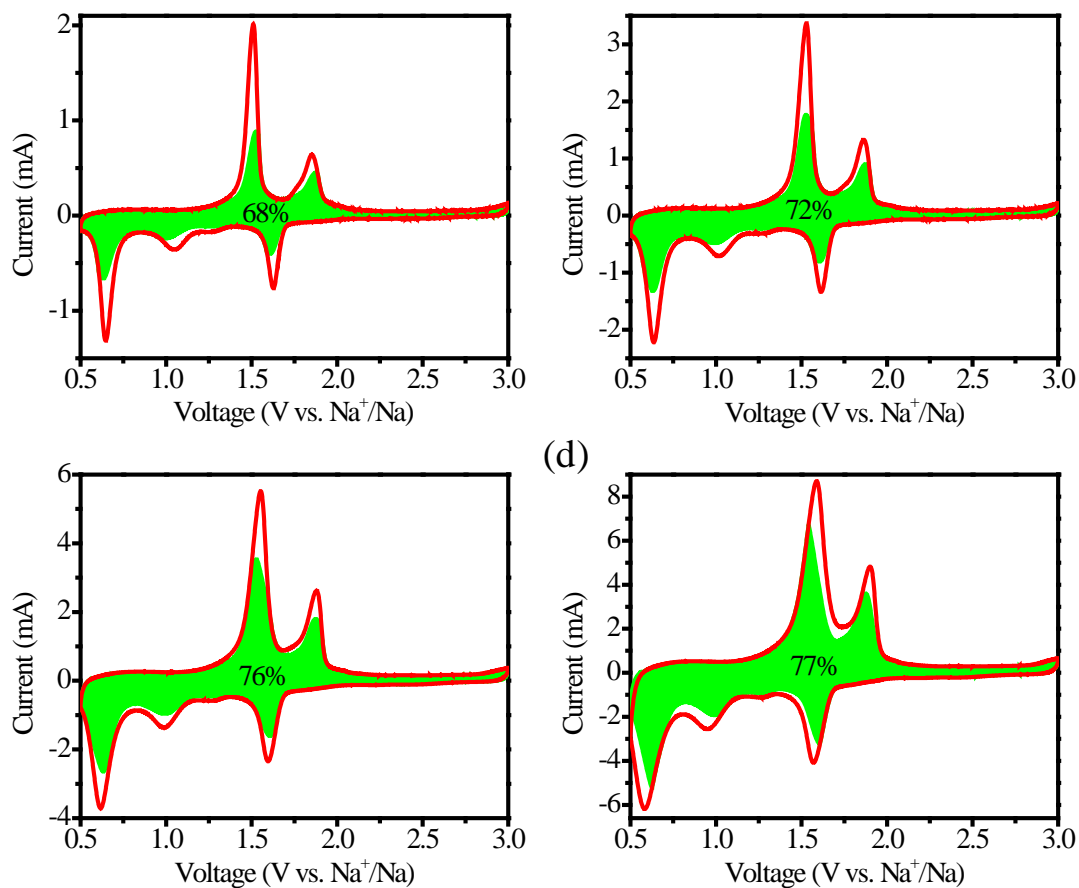


Figure S12. Capacitive contributions (shaded area) at the scanning rate of (a) 0.4, (b) 0.8, (c) 1.6 and (d) 3.2  $\text{mV s}^{-1}$ .

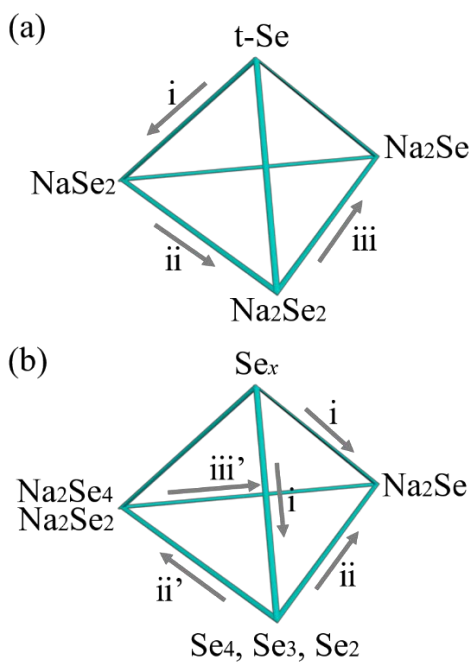


Figure S13. Possible sodiation mechanism of (a) trigonal Se and (b) amorphous  $\text{Se}_x$  chains.

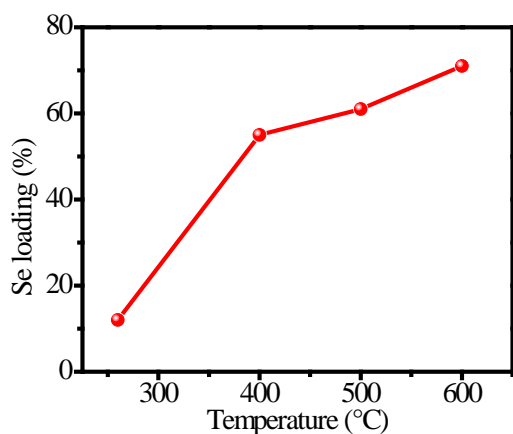


Figure S14. Temperature dependence of selenium loading for the vapor-infiltration method.

Table S1. Comparative Na-Se battery performance review of recently reported Se/C composites

Material	Fabrication method	Se loading	Electrolyte	Capacity mAh g <sup>-1</sup> (A g <sup>-1</sup> )	Se Capacity mAh g <sup>-1</sup> (A g <sup>-1</sup> )	Initial CE	Ref
VSeG	Vapor-infiltration	71%	DEGDME	410(0.1) 367(1)	577(0.14) 517(1.4)	88%	This work
SeCT	vacuum-calcination	52%	PC	317(0.035) 265(0.35)	601(0.068) 510(0.68)	55%	1
CNF/Se	melt-infusion	72%	EC/DMC	432(0.049) 360(0.244)	578(0.068) 500(0.34)	74%	2
Se-NCMC	melt-infusion	70%	EC/DMC	358(0.048) 210(0.48)	511(0.068) 310(0.68)	58%	3
Se@MCNF	melt-infusion	48%	EC/DEC	298(0.048) 182(0.96)	621(0.1) 379(2)	72%	4
Se/NCPCs	melt-infusion	49%	EC/DEC	212(0.033) 159(0.33)	437(0.068) 328(0.68)	45%	5
Se-CNN	melt-infusion	53%	EC/DMC	325(0.036) 188(0.36)	613(0.068) 355(0.68)	64%	6

DEGDME: diethylene glycol dimethyl ether; PC: propylene carbonate; EC: ethylene carbonate; DEM: dimethyl carbonate; DEC: diethyl carbonate; CE: coulombic efficiency

### References:

(1) Yang, X.; Wang, H.; Yu, D. Y. W.; Rogach, A. L. Vacuum Calcination Induced Conversion of Selenium/Carbon Wires to Tubes for High-Performance Sodium–Selenium Batteries. *Adv. Funct. Mater.* **2018**, *28*, 1706609.

- (2) Wang, H.; Jiang, Y.; Manthiram, A. Long Cycle Life, Low Self-Discharge Sodium-Selenium Batteries with High Selenium Loading and Suppressed Polyselenide Shuttling. *Adv. Energy Mater.* **2018**, *8*, 1701953.
- (3) Ding, J.; Zhou, H.; Zhang, H.; Tong, L.; Mitlin, D. Selenium Impregnated Monolithic Carbons as Free-Standing Cathodes for High Volumetric Energy Lithium and Sodium Metal Batteries. *Adv. Energy Mater.* **2017**, *8*, 170198.
- (4) Yuan, B.; Sun, X.; Zeng, L.; Yu, Y.; Wang, Q. A Freestanding and Long-Life Sodium–Selenium Cathode by Encapsulation of Selenium into Microporous Multichannel Carbon Nanofibers. *Small* **2017**, *14*, 1703252.
- (5) Xu, Q.; Liu, T.; Li, Y.; Hu, L.; Dai, C.; Zhang, Y.; Li, Y.; Liu, D.; Xu, M. Selenium Encapsulated into Metal–Organic Frameworks Derived N-Doped Porous Carbon Polyhedrons as Cathode for Na–Se Batteries. *ACS Appl. Mater. Interfaces* **2017**, *9*, 41339-41346.
- (6) Ding, J.; Zhou, H.; Zhang, H.; Stephenson, T. J.; Li, Z.; Karpuzov, D.; Mitlin, D. Exceptional Energy and New Insight with Sodium–Selenium Battery Based on Carbon Nanosheet Cathode and Pseudographite Anode. *Energy Environ. Sci.* **2016**, *10*, 153-165.